Direct visualization of quasi-ordered oxygen chain structures on Au(110)-(1×2)

Direct visualization of quasi-ordered oxygen chain structures on Au(110)-(1x2)

F. Hiebel[1], M. M. Montemore[1,2], E. Kaxiras[2,3], C. M. Friend[1,2,*]

1. Department of Chemistry and Chemical Biology, Harvard University, Cambridge MA 02138

2. School of Engineering and Applied Sciences, Harvard University, Cambridge MA 02138

3. Department of Physics, Harvard University, Cambridge, Massachusetts 02138

* Corresponding author at: friend@fas.harvard.edu

Abstract

The Au(110) surface offers unique advantages for atomically-resolved model studies of catalytic oxidation processes on gold. We investigate the adsorption of oxygen on Au(110) using a combination of scanning tunneling microscopy (STM) and density functional theory (DFT) methods. We identify the typical (empty-states) STM contrast resulting from adsorbed oxygen as atomic-sized dark features of electronic origin. DFT-based image simulations confirm that chemisorbed oxygen is generally detected indirectly, from the binding-induced electronic structure modification of gold. STM images show that adsorption occurs without affecting the general structure of the pristine Au(110) missing-row reconstruction. The tendency to form one-dimensional structures is observed already at low coverage (<0.05ML), with oxygen adsorbing on alternate sides of the reconstruction ridges. Consistently, calculations yield preferred adsorption on the (111) facets of the reconstruction, on a 3-fold coordination site, with increased stability when adsorbed in chains. Gold atoms with two oxygen neighbors exhibit enhanced electronic hybridization with the O states. Finally, the species observed are reactive to CO oxidation at 200K and desorption of CO_2 leaves a clean and ordered gold surface.
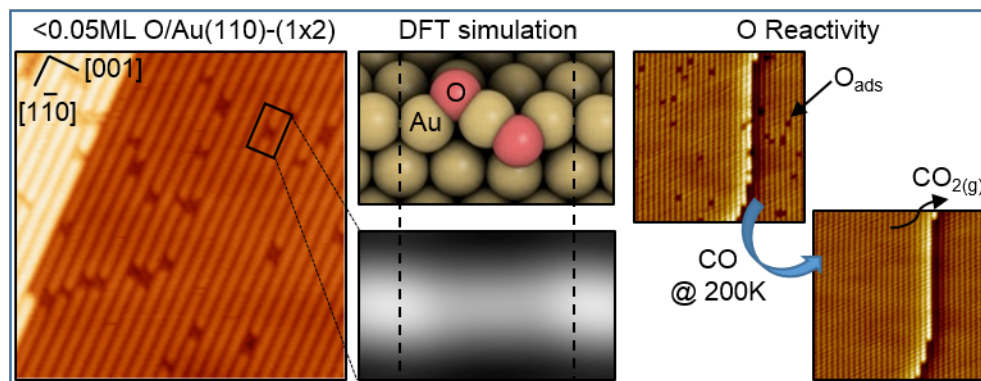
1. Introduction

Visualization of reactive adsorbed species is a powerful tool for understanding how chemical reactions occur on surfaces, especially in heterogeneous catalysis.[1] Prof. Madix, who is being honored by this special issue, was a pioneer in the application of scanning tunneling microscopy (STM) to the investigation of chemical reactions on surfaces, including coinage metals.[2] Because gold is an efficient and selective catalyst for oxidation processes[3-9] there is considerable interest in imaging reactant species, including adsorbed oxygen (O_{ads}), on its surfaces. Model studies on single crystal surfaces[10-13] provide a mechanistic understanding of how oxidative processes are promoted on Au,[14] with the final goal of predicting new reactions.[15] To date, the majority of mechanistic studies have focused on O-covered Au(111), which roughens upon O atom adsorption[16] even at low coverage (0.1ML) and low temperature (~200 K).[17] The roughening of the surface associated with oxygen adsorption limits our ability to use STM because it is not possible to visualize adsorbates at the atomic scale. If a more well-ordered system state of adsorbed O were accessible that had the same reactivity, the high spatial resolution offered by STM could be used to probe the details of adsorbate organization and overall reactivity.

Atomic visualization of the states of O adsorption on gold is of particular interest because its reactivity depends strongly on coverage and on the degree of order. DFT results coupled with studies of the vibrational properties of O adsorbed on Au(111) provide evidence that the local bonding environment depends on coverage.[18] While at low coverage and low temperature a disordered surface is observed, STM demonstrates that ordered oxide islands form at high O coverage.[17] The activity for CO oxidation on O-covered Au(111) at 200K is a factor of ~3 times faster for the disordered low O coverage surface compared to the ordered surface oxide at half saturation.[17] In addition, the activity and selectivity for O-assisted methanol coupling on O-covered Au(111) depends on O coverage—higher activity and selectivity are observed for low O coverages. [19]

Herein, we investigate the bonding of O on Au(110) in order to better exploit atomic-scale imaging using STM in conjunction with DFT studies. The Au(110) surface reconstructs to the missing-row Au(110)-(1x2) structure, which consists of an ordered array of (111) microfacets[20-22] capped by rows of atoms with low coordination number along the [1-10] direction (Fig. 1a). Where comparable studies have been performed, the reactivity of O-covered

2

Au(110)-(1x2)[23] and Au(111)[19] are similar. Likewise, the temperatures for O recombination to O_2 are similar for the (111)[24,25] and (110)[26] surfaces.

Previous electronic structure calculations suggest that O bound to Au(110) is most stably bound in pseudo-threefold sites (Fig. 1),[27] similar to the binding geometry for O on Au(111).[28,29] At higher O coverage, the formation of anti-symmetric chain-like structures are predicted (Fig. 1).[30] These studies motivated our quest to image atoms of O on Au(110)-(1x2) at the atomic scale in order to better understand O-Au bonding. We find that O is generally imaged indirectly through the electronic perturbations induced in its gold nearest neighbors and this result is corroborated by simulated STM images. When the oxygen atoms are directly imaged, anti-symmetric chain-like structures are revealed. Multi-oxygen features are prevalent already at low coverage and computational results indicate stabilization of the oxygen upon chain formation. At low coverage, the oxygen species do not induce strong surface reconstruction and they are reactive for CO oxidation, which makes this system amenable to studying oxidation reactions on gold at the atomic scale using STM.
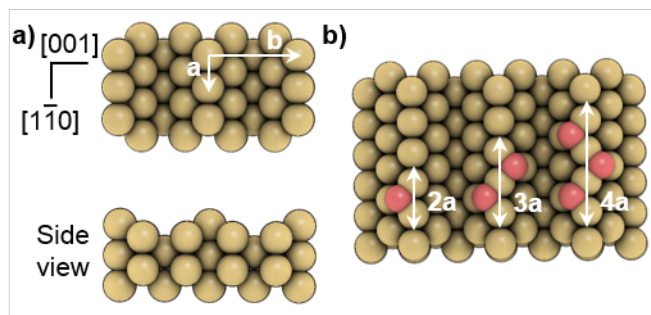

Figure1: (a) Schematic of the bare Au(110)-(1x2) surface reconstruction (top and side view). The surface periodic vectors shown by arrows are a=2.88 Å and b=8.16 Å. (b) Schematic of the oxygen (red) adsorption geometry at coverage ≤0.25ML based on the antisymmetric chain model.[27,30]

2. Methods

Experimental. The Au(110) single crystal was purchased from Princeton Sci. and cleaned via cycles of sputtering and annealing at ~900K until no impurity trace was detected by Auger electron spectroscopy, and STM showed a uniform Au(110)(1x2) surface. Atomic O was created by exposing the surface to ozone since O_2 does not measurably dissociate on crystalline gold.[10,12] Directed ozone dosing was performed using a continuous flow from an ozone generator (Ozone Engineering, model LG-7) to the 1 cm-diameter doser, located ~2 mm from the sample surface. Prior to experiments, several cycles of ozone dosing/annealing were

performed to ensure a clean dosing line and sample surface. During exposure, the sample was kept at room temperature. Temperature programmed desorption (TPD) experiments confirm the adsorption of oxygen. At low oxygen coverage, a single desorption peak at ~550 K is observed (Fig. S1), in agreement with previous studies [31] which also determined that saturation of this peak corresponds to one monolayer (ML) of oxygen (4 atoms per Au(110)-(1x2) unit cell[21]). Prior to STM experiments, the samples were mildly annealed to ~450K for 5 min. The oxygen deposition on the surface was first calibrated by TPD and the amount of oxygen on the surface was verified via TPD post STM experiments. STM experiments were conducted under base pressure below 1.0 x 10^{-10}mbar using an Omicron VT-STM and mechanically cut Pt-Ir tips. Typical scanning rate was 200-500 nm/s, bias voltage between -1.5 V and 1.5 V and low tunneling current of 0.1-0.2 nA. Imaging was mostly performed at a low temperature of ~150 K. While some oxygen mobility was detected at 300K, it did not prevent clear images.

Computational. Plane-wave DFT calculations were performed using VASP.[32,33] The PW91 exchange-correlation functional was used, along with the projector-augmented wave method,[34,35] a 396 eV cutoff energy, and a 5x7x1 k-point grid. The supercell consisted of a 4x2 Au(110)-(1x2) surface cell with 8 layers, with the bottom 6 fixed in their bulk positions. Approximately 20 Å of vacuum space were included in order to avoid artifacts on the calculated density of states contours. Simulated STM images were generated based on the Tersoff-Hamann theory,[36] as implemented in the bSKAN package.[37] They consist of maps of constant density of states integrated over [E_F;E_F+1.5eV]. bSKAN and its interface with VASP allowed us to easily obtain accurate, noise-free contours far from the surface. Atomic graphics were created in QuteMol[38] and Vesta.

3. Results and discussion

STM contrast on oxygen on Au(110) and its origin. Oxygen atoms bound to Au(110)-(1x2) generally appear as dark features on the surface row structure in STM images obtained using positive bias (Fig. 2). We mainly concentrate on the empty-states (V>0) contrast since those imaging conditions provide the most reproducible contrast. Dramatic changes in contrast associated with the tip state when imaging filled-states (V<0) however provide useful information as will be discussed in connection with Fig. 3. The STM contrast on pristine Au(110)-(1x2)[20] consists of continuous rows in the [1-10] direction with a 0.5 Å corrugation amplitude in the [001] direction and 1.4 Å high atomic steps (Fig. 2a, left panel). Upon O adsorption, besides the appearance of dark features, the surface reconstruction is generally unaltered, as seen in Fig. 2a for O coverage of 0.025±0.005 ML. The length of the dark features

4

along the [1-10] direction can be indexed in terms of the Au lattice constant as (2+n) a with n=0, 1, 2... and a=2.88Å, the lattice constant along the close-packed direction (Fig. 2b). The smallest (2-cell) features have an apparent depth of 0.54±0.02 Å, whereas longer ones appear to be 0.61±0.03 Å deep relative to the top-most gold atoms (Fig. 2c). The small corrugation of these features compared to the bare surface step height (1.4 Å) suggests that the corrugation is an electronic effect, as opposed to pure topography. This assertion is addressed both experimentally and theoretically.
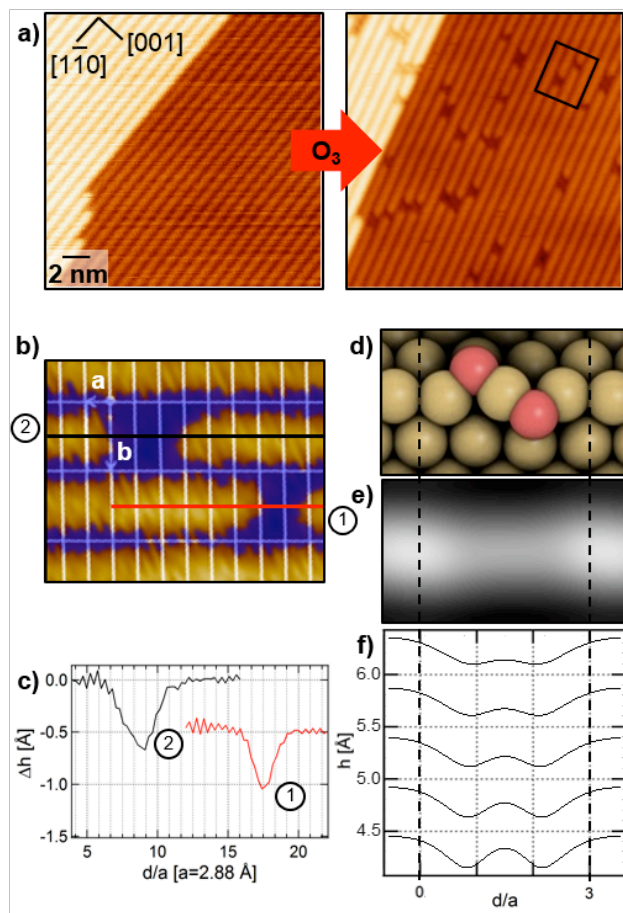

Figure 2: STM signature of low-coverage O species. (a) evolution from clean Au(110)-(1x2) (20x20 nm^2 image; V_s=0.1 V; I_t=0.1 nA). to 0.025±0.005 ML O-covered Au(110)-(1x2) (20 x20 nm^2; V_s=+1.5V; I_t=0.2nA); (b) magnified view of boxed area in (a) The blue color cutoff corresponds to the average half-depth of the dark features. (c) Profiles in the row direction across the oxygen features in (b). (d) DFT-calculated geometry (e) DFT-simulated empty-states STM (tip-surface distance ~6 to 6.5 Å) (f) Contours of constant density of states integrated over [E_F; E_F+1.5eV], across the topmost gold atoms in the direction of the rows at various distances from the surface. Experimentally, the contour followed by the tip is governed by the tunneling current: the lower the set-point current, the farther from the surface.

DFT calculations determine the lowest energy configuration and also confirm that the decrease in tunneling current observed experimentally is due to the nature of the O-Au bonding. The lowest energy configuration obtained corresponds to O bound to pseudo-3-fold sites on opposite sides of a ridge of gold atoms (Figs. 1b, 2d), in agreement with previous work.[30] This structure is consistent with the length of (2+n)a of features along the [1-10] direction, as

5

determined by STM. Within this structure model, features with n>2 darker gold atoms contain (n-2) atoms that are perturbed by *two* oxygen atoms. This would explain the slightly deeper features compared to the ones we associate with one oxygen atom. The oxygen adsorption structure and resulting electronic interactions are discussed in more detail below. When considering a 2-atom oxygen chain model (Fig. 2d), contours of constant density of empty states reproduce the depression above the gold atoms bonded to oxygen for tip-sample distance >5 Å (Fig. 2f), which is consistent with experimental estimates of this distance.[20] A more detailed analysis of the signal detected closer to the surface on the center gold atom is provided in the supplemental material (Figs. S2, S5b).

Simulation of the empty-state STM image for a tip-surface distance of ~6 to 6.5 Å using the DFT results shows that the O feature presents mirror symmetry with respect to the [1-10] direction (Fig. 2e), as in STM (Fig. 2c). Consistent with STM, this suggests that any topographic change due to the oxygen adatoms is not detectable for this energy range and tip-surface distance. The oxygen adatom is located in the surface trough, ~0.1Å higher than the topmost gold atoms.[30] Hence, the topographic modulation is compensated by the electronic effect identified in our calculations, i.e. the perturbation in the electronic structure of gold by the adsorbed oxygen. There is precedent for oxygen adsorbed on transition metals appearing as depressions under positive bias in both experimental and theoretical studies. For example, low-temperature O adsorbed in the Ag(110) troughs is imaged as a depression[39] and this contrast was reproduced using similar STM simulations.[40]

The experimental STM contrast associated with the presence of adsorbed O strongly depends on the sample voltage and tip state and even vanishes in certain tunneling conditions, further establishing that the corrugation is mostly electronic in nature. Two constant-current images obtained simultaneously (forward/backward trace) with sample biases of +1.5 V and -1.5 V demonstrate this effect (Fig. 3a). The +1.5 V image exhibits the typical darker contrast attributed to the presence of O (0.14±0.01 ML coverage). On the -1.5 V image, this contrast is vanishingly small. At +1.5 V, the dark areas and the areas attributed to unperturbed gold show a 0.73 Å height difference. At -1.5 V, this difference is nearly undetectable. Additionally, comparing images at various positive sample biases shows that the corrugation on the O-features decreases with sample bias (Fig. S3). This is also supported by I(V) mapping of the surface (Fig. S4).
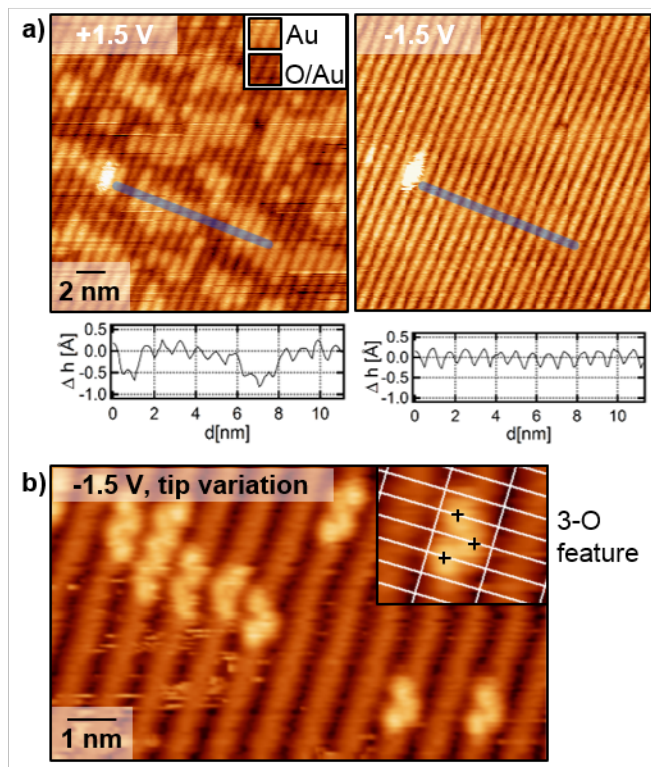
6

Figure 3: *Bias- and tip-dependent contrast on the O-related features demonstrates the electronic nature of the corrugation. (a) 0.14±0.01 ML O surface, simultaneous images (20x20 nm^2) obtained for positive (left) and negative (right) bias (V_s=+/-1.5 V; I_t=0.1 nA, T= 150 K) and the corresponding profiles across the blue lines (below). (b) 0.03±0.01 ML O coverage surface. A tip variation reveals the O atoms at negative sample bias, bright protrusion ordered into zig-zag structures appear (10x6 nm^2; V_s=-1.5 V; I_t=0.2 nA, T= 150 K). Inset: bottom right feature, together with the surface reconstruction lattice.*

Oxygen adsorption structure. STM reveals that the tendency for O to form one-dimensional multi-O structures exists already at low coverage (Fig. 2). A low temperature measurement for 0.02 ML O coverage shows that isolated O features amount to only 9% of 367 features measured (Fig. S7). In agreement with this measurement, we calculate a stronger adsorption for a second O atom in the chain. In the convention of negative adsorption energy for binding interactions, the adsorption energy is lowered from -3.67 eV for the first O atom to -3.81 eV for the second (relative to the O in the gas phase) on the 2O-structure in Fig. 2e.

Aside from bias-dependent variations presented (Fig.3), the tip state can also alter the O-related contrast, and even reveal the O atoms hence providing useful information on their adsorption structure. The dark features most commonly observed in positive bias (Fig. 2) are sometimes detected in negative sample bias images, and can also disappear almost completely on positive sample bias images (Fig. S5a). Contrast variations with the tip state are typical of features of electronic origin. Interestingly, on rare occasions, it is possible to image protrusions on alternate sides of the topmost Au row, forming small chains along the [1-10] direction (Fig. 3b). Note that we only observed this behavior at negative sample bias and it is thus not in contradiction with

the simulations for positive bias imaging. In the literature, a tip-dependent inversion of contrast on O on Pt(111) has been reported in some tip conditions[41] and simulations including contamination of the tip were able to reproduce it.[42] We propose that in our case, the protrusions correspond to the O adatoms, and that these can be imaged when the tip is contaminated, most probably with O. Note also that the protrusions appear when imaging the surface filled-states, for an energy window encompassing the O 2p-derived resonance on gold, as seen in Fig. 4. In this light, the features in Fig. 3b are consistent with the asymmetric chains structure model depicted in Fig. 1b.

DFT calculations provide insight into local O-induced atomic and electronic structure modifications of the surface within an O chain. In the two-O chain structure in Fig. 4a, atoms in the topmost row binding to O are considered, atom 1 and 1'are binding to one O and atom 2 is binding to two O. Structurally, atoms 1 and 1' have moved by 0.1 Å outward from the surface, while the central atom undergoes a larger displacement of 0.6 Å. Additionally, the top view in Fig. 4b shows that atoms 1 and 1' move 0.2 Å away from atom 2 in the row direction which represents ~7% increase in the interatomic distance. In the direction perpendicular to the rows, they show 0.1 Å displacement away from the O atom and the structure is symmetric with respect to the central Au atom. Au atom 2 transfers significantly more charge (Bader[43] charge +0.45 e) to O (Bader charge -0.74 e) than Au atoms 1 and 1' (Bader charge +0.15), as depicted in Figs. 4a,b. The comparison between projected density of filled states on Au atoms 1 and 2 and that on clean Au shows electronic states hybridization between the O and Au states (Fig. 4c-e) with an increased weight on both sides of the Au d band and the appearance of a sharp resonance close to -6 eV characteristic of O. Importantly, the electronic states hybridization is enhanced for the Au atom binding to two O (atom 2) with respect to an Au atom binding to one O (Atoms 1,1'), that is, at the end of a chain (Fig. 4) This result is similar to what has been recently reported for O adsorption on Au(321).[44] We note here that the antisymmetric geometry probably is favored because it allows a larger distance between the O adatoms and screening of their charge by the Au row. The structure also allows equilibrium in alternating displacement of the topmost atoms in the direction perpendicular to the rows. In the case of O chains on Ag(110), the ordering of the O and their mutual stabilization impacts oxidation reaction rates.[45,46] Although, as discussed in the following, the exact chain structure is different, similar end effects could be expected on Au(110).
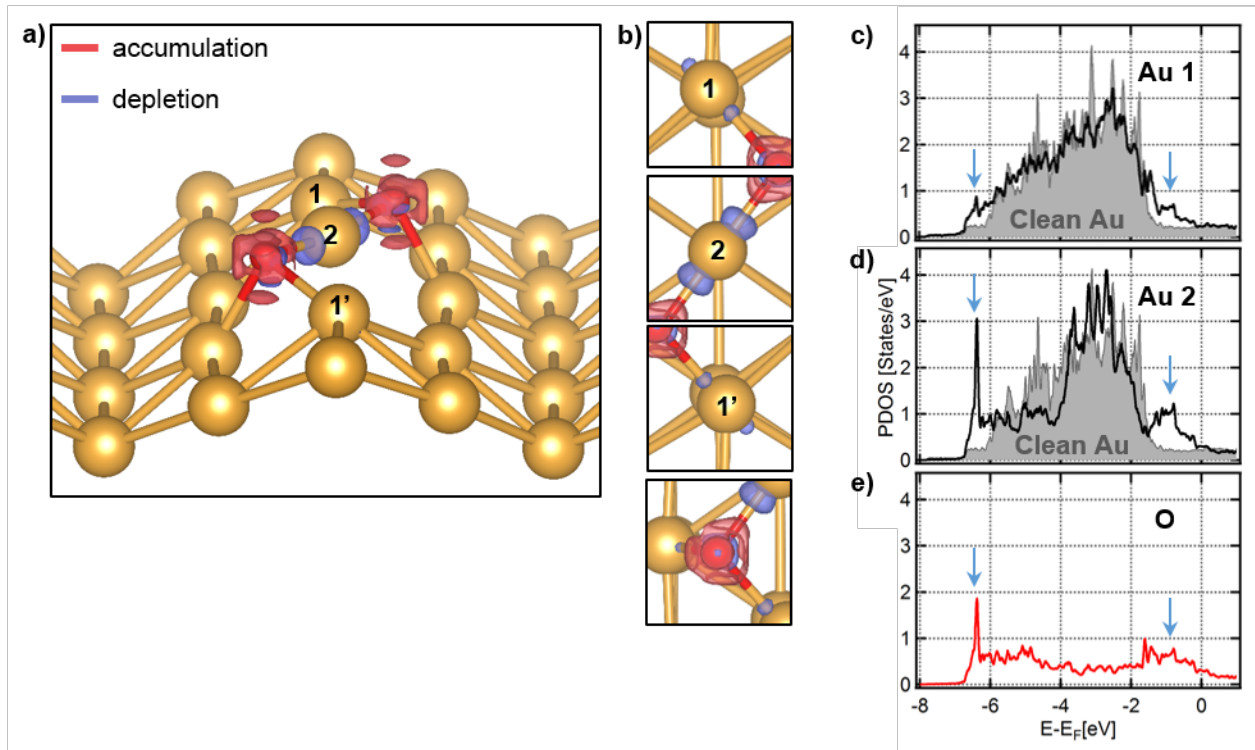
8

Figure 4: *Two-O relaxed structure together with charge density difference isosurfaces and projected density of states (PDOS) on Au atoms and O adatom. (a) Perspective side view, and (b) top view of the relaxed structure together with the O-induced charge accumulation and depletion (isosurface values ±0.02 e/Å³). PDOS on the topmost Au atoms binding to O compared to topmost Au atom in the clean structure. (c) Au with 1 O neighbor (atom 1 in (a)); (d) Au with 2 O neighbors (atom 2 in (a)); (e) PDOS on O. For symmetry reasons, both O (1 and 1') atoms show the same PDOS. Arrows indicate PDOS features that are common in both Au and O, indicating electronic state hybridization. O-Au hybridization appears to be stronger for the Au with 2 O neighbors than the Au with 1 O neighbor.*

In order to understand how O can adsorb on Au(110) without inducing strong structural perturbations, we compare gold and silver in their response to O adsorption. Regarding the clean surfaces, it is known that the transition from 4d to 5d has important structural implications. While pure Ag(110) adopts a (1x1) surface structure, the Au(110) surface reconstructs. In the reconstruction, the total amount of Au-Au bonds is unchanged compared to the ideal surface but the total energy is reduced by redistributing them into a richer variety of coordination numbers.[47,48] Relativistic effects are important in Au[27,49] but not Ag, and the stability of the Au reconstruction has been explained by overall contraction of the s electrons and their

enhanced extension into the vacuum at the surface, both of which allow a larger d-orbital overlap between metal atoms.[48,50,51] When exposing Ag(110) to dioxygen at T>200 K,[52,53] metal atoms are incorporated into an added-row structure of Ag-O-Ag chains along the [001] direction.[54-56] Generally, surfaces reconstruct upon adsorption if the gain in adsorption energy on the reconstructed surface compensates the cost of the reconstruction.[47] The cost of breaking Ag-Ag bonds is compensated by the gain in chemisorption energy through enhanced electronic interaction between O and under-coordinated metal atoms.[57] Because gold shows a stronger metal-metal bond due to strong 5d bonds and a weaker O-metal bond, we expect it to respond differently to O adsorption. Theoretical investigations of O adsorption on Au(110) show stabilization of the adsorbate on the missing-row surface as opposed to adsorption on the (1x1) surface,[27] up to 0.5ML when forming chain-like structures.[30] The reported optimum adsorption site involves two topmost Au atoms of the (1x2), similarly to the tendency for O to adsorb close to defects with under-coordinated atoms on Au(111).[28,29] On the missing-row reconstruction, no creation of defects is required to allow O to interact with under-coordinated Au atoms, at least until maximum coordination for the topmost Au atoms is reached at 0.5ML of O.[30] Consistently, we observe the onset of atomic roughness around this coverage for the as-deposited surface (Fig. S6). Additionally, the (1x2) structure is still detected up to at least 0.75 ML of O in our low energy electron diffraction (LEED) measurements (not shown). Consistently with the literature,[26,58] we however observe a progressive increase in background intensity. The background signal below 0.5 ML of O could be explained by the limited extension of the O chains, their weak ordering (discussed below) and their small mobility at room temperature together with the above presented induced distortions in the Au surface.

For sufficiently high coverage, the non-random distribution of the O chains becomes apparent. For high coverage but below 0.25 ML which corresponds to saturation coverage for the antisymmetric chain geometry (e.g. ~0.15ML in Fig. 3a), the surface shows O chains that are limited to a few nm in length i.e. in the Au row direction. Loose ordering of those chains results in a nanopattern consisting of alternate bright/dark stripes of a few nm in width in the direction of the Au rows and several tens of nm in the direction perpendicular to the Au rows. It is known that stress relaxation can lead to the patterning of surfaces in the nm scale, e.g. Au(111) ordering into the characteristic herringbone pattern.[59] Given the O-induced mild atomic structure perturbations indicated by our DFT calculations, it is relevant to consider a similar origin to the O-Au(110) surface nanopattern. In fact, O adsorption on the missing-row Pt(110)-(1x2) surface leads to analogous nanopatterns, which was proposed to arise from stress relief through lattice relaxation along the ridges.[60] Our calculations yield an increase of interatomic

10

spacing by ~7% in the Au ridges where O is adsorbed (Fig. 4f), which is of the same order as the 5% reported lattice expansion within O chains on Pt(110); the Pt(110) surface lattice parameter in the row direction is 2.78 Å which is close to 2.88 Å for gold. The nanopatterns formed upon O adsorption could thus have the same origin on both surfaces. Interestingly, elastic relaxation has been invoked in order to explain the repulsive interaction between Ag-O chains on Ag(110) in the direction of the Ag rows ([1-10]).[61-63] Further studies on the quasi-ordering of the chains below roughening coverage and its impact on reactivity are planned.

Reactivity of the oxygen species. The oxidation of CO by the O adsorbed on Au(110) demonstrates that the features observed in STM are, indeed, due to O and also that there is no Au atom incorporation into the O structures. Exposure to CO removes the dark features, leaving a clean Au(110)-(1x2) surface with no obvious restructuring of the step edges (Fig. 5). CO is known to react with O adsorbed on Au(110), even below room temperature.[64] In the example shown, the temperature (200K) was chosen so as to suppress the mobility of the O, demonstrated by the correspondence of images taken before and after a short exposure of the O-covered Au(110) to CO (Figs. 5a, b). At the same time, the temperature is sufficiently high that there is no accumulation of either CO or of the CO_2 product.[65] Approximately a third of the O is removed after exposure to ~10L of background CO at 200 K. Initially, there are 28 features related to O_{ads} compared to 19 features after exposure to CO (Figs. 5a,b respectively). After ~1000L of CO, no adsorbed O remains and the image is the same as the initially clean surface; notably, there is no restructuring of the step edge. Note that because of the close proximity of the tip to the surface, a much lower effective CO pressure than the measured background pressure is expected in the field of imaging. Here we present qualitative results; the kinetics of CO oxidation on O-activated Au(110) have been investigated in detail with reactive thermal desorption measurements by Gottfried *et al*.[64,65] The disappearance of the dark features upon exposure to CO is strong supporting evidence that the dark features are caused by the presence of O adatoms. After the reaction, the typical contrast for pristine gold is restored (see blue arrow on Figs. 5a,b). We show here that the O species we observe are reactive and that they form without strong restructuring of the gold surface, unlike O on the Au(111) surface. The CO oxidation itself also does not induce strong restructuring of the gold surface.
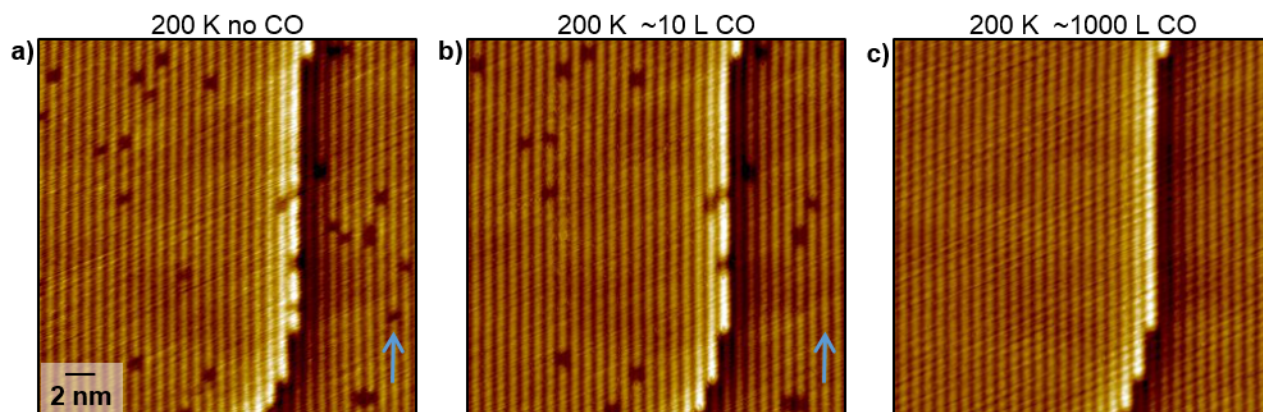
11

Figure 5: *Reactivity of O towards CO at 200K, 0.02-0.03 ML initial O coverage. 25x25nm^2 STM images (Vs=+1.5V; It=0.2nA, the images have been flattened in order to show both terraces and the step edge appears brighter.) (a) no CO, (b) 12 minutes at 1×10^{-8} mbar (c) 3.75 hours at average background pressure 0.7×10^{-8} mbar. Imaging time: 60 s. The O features are progressively cleaned off (see arrow).*

4. Conclusion

Using a combination of experimental (STM) and theoretical (DFT) tools, we have provided a detailed interpretation of the STM contrast and identified the O adsorption site and multi-O structures for low-coverage O on Au(110). O is mostly detected indirectly on empty-states images, through the reduced density of states on its direct Au neighbors, as reproduced by STM images simulated with DFT. Low coverage of O does not induce strong restructuring of the gold surface. STM results are consistent with adsorption on the (111) facets of the reconstruction, on a 3-fold coordinated site involving two undercoordinated topmost gold atoms. We unequivocally demonstrate that O atoms form asymmetric chains even at low coverage, which to our knowledge had only been studied theoretically in the literature. Within the chains, topmost gold atoms are binding with two O atoms and our calculations show a stabilization of the system together with an increased Au-O electronic hybridization. The ability to clearly identify O structures at the atomic scale opens new possibilities for atomically resolved studies of catalytic oxidation on gold. We have presented, in a proof-of-principle experiment, that the O species observed are reactive to CO oxidation. Probing the interplay between the O adsorption structure

12

and its reactivity would be one particular interesting direction for future investigations, since computations indicate a stabilization of the O within the chains.

References

[1] W. Ho, J. Chem. Phys. 117 (2002) 11033-11061.

[2] X.C. Guo, R.J. Madix, J. Phys. Chem. B 107 (2003) 3105-3116.

[3] M. Haruta, Angew. Chem. Int. Ed. 53 (2013) 52-56.

[4] L. McEwan, M. Julius, S. Roberts, J. Fletcher, Gold Bull. 43 (2010) 298-306.

[5] C. Della Pina, E. Falletta, M. Rossi, Chem. Soc. Rev. 41 (2012) 350-369.

[6] Y. Zhang, X. Cui, F. Shi, Y. Deng, Chem. Rev. 112 (2011) 2467-2505.

[7] X. Liu, L. He, Y.M. Liu, Y. Cao, Acc. Chem. Res. 47 (2013) 793-804.

[8] X. Zhang, Y. Ding, Catal. Sci. Technol. 3 (2013) 2862-2868.

[9] A. Wittstock, M. Baumer, Acc. Chem. Res. 47 (2014) 731-739.

[10] S. Carabineiro, B.E. Nieuwenhuys, Gold Bull. 42 (2009) 288-301.

[11] S. Carabineiro, B.E. Nieuwenhuys, Gold Bull. 43 (2010) 252-266.

[12] J. Gong, Chem. Rev. 112 (2011) 2987-3054.

[13] M. Pan, J. Gong, G. Dong, C.B. Mullins, Acc. Chem. Res. 47 (2014) 750-760.

[14] K.J. Stowers, R.J. Madix, C.M. Friend, J. Catal. 308 (2013) 131-141.

[15] B. Xu, R.J. Madix, C.M. Friend, Acc. Chem. Res. 47 (2014) 761-772.

[16] B.K. Min, X. Deng, D. Pinnaduwage, R. Schalek, Phys. Rev. B 72 (2005) 121410.

[17] B.K. Min, A.R. Alemozafar, D. Pinnaduwage, X. Deng, C.M. Friend, J. Phys. Chem. B 110 (2006) 19833.

[18] T.A. Baker, B. Xu, X. Liu, E. Kaxiras, C.A. Friend, J. Phys. Chem. C 113 (2009) 16561-16564.

[19] B. Xu, X. Liu, J. Haubrich, R.J. Madix, C.M. Friend, Angew. Chem. Int. Ed. 48 (2009) 4206.

[20] G. Binnig, H. Rohrer, C. Gerber, E. Weibel, Surf. Sci. Lett. 131 (1983) L379-L384.

[21] W. Moritz, D. Wolf, Surf. Sci. Lett. 163 (1985) L655.

[22] D.D. Dos Reis, F.R. Negreiros, V.E. De Carvalho, E.A. Soares, Surf. Sci. 604 (2010) 568.

[23] D.A. Outka, R.J. Madix, J. Am. Chem. Soc. 109 (1987) 1708-1714.

[24] N. Saliba, D.H. Parker, B.E. Koel, Surf. Sci. 410 (1998) 270-282.

[25] K.A. Davis, D.W. Goodman, J. Phys. Chem. B 104 (2000) 8557-8562.

[26] J.M. Gottfried, K.J. Schmidt, S.L.M. Schroeder, K. Christmann, Surf. Sci. 511 (2002) 65.

[27] M. Landmann, E. Rauls, W.G. Schmidt, Phys. Rev. B 79 (2009) 045412.

[28] Z.P. Liu, P. Hu, A. Alavi, J. Am. Chem. Soc. 124 (2002) 14770.

[29] T.A. Baker, C.M. Friend, E. Kaxiras, J. Phys. Chem. C 113 (2009) 3232-3238.

[30] M. Landmann, E. Rauls, W.G. Schmidt, J. Phys. Chem. C 113 (2009) 5690.

[31] J.M. Gottfried, K.J. Schmidt, S.L.M. Schroeder, K. Christmann, Surf. Sci. 525 (2003) 184.

[32] G. Kresse, J. Furthmüller, Comput. Mater. Sci. 6 (1996) 15-50.

[33] G. Kresse, J. Hafner, Phys. Rev. B 47 (1993) 558-561.

[34] P.E. Blöchl, Phys. Rev. B 50 (1994) 17953-17979.

[35] G. Kresse, D. Joubert, Physical Review B 59 (1999) 1758-1775.

[36] J. Tersoff, D.R. Hamann, Phys. Rev. B 31 (1985) 805-813.

[37] K. Palotás, W.A. Hofer, J. Phys. Condens. Matter 17 (2005) 2705-2713.

[38] M. Tarini, P. Cignoni, C. Montani, IEEE Trans. Vis. Comput. Graphics 12 (2006) 1237-1244.

[39] J.R. Hahn, W. Ho, Phys. Rev. Lett. 87 (2001) 166102.

[40] F.E. Olsson, N. Lorente, M. Persson, Surf. Sci. Lett. 522 (2003) L27-L35.

[41] B.C. Stipe, M.A. Rezaei, W. Ho, S. Gao, M. Persson, B.I. Lundqvist, Phys. Rev. Lett. 78 (1997) 4410.

[42] M.L. Bocquet, J. Cerda, P. Sautet, Phys. Rev. B 59 (1999) 15437-15445.

[43] W. Tang, E. Sanville, G. Henkelman, J. Phys. Condens. Matter 21 (2009) 084204-084211.

[44] L.V. Moskaleva, T. Weiss, T. Klüner, M. Bäumer, J. Phys. Chem. C 119 (2015) 9215.

14

[45] J.T. Ranney, S.R. Bare, Surf. Sci. 382 (1997) 266-274.

[46] O. Nakagoe, K. Watanabe, N. Takagi, Y. Matsumoto, J. Phys. Chem. B 109 (2005) 14536.

[47] J.K. Nørskov, Surf. Sci. 299 (1994) 690-705.

[48] K.M. Ho, K.P. Bohnen, Phys. Rev. Lett. 59 (1987) 1833-1836.

[49] S. Olivier, G. Tréglia, A. Saúl, F. Willaime, Surf. Sci. 600 (2006) 5131-5135.

[50] A. Nduwimana, X.G. Gong, X.Q. Wang, Appl. Surf. Sci. 219 (2003) 129-135.

[51] R. Smit, C. Untiedt, A.I. Yanson, J.M. Van Ruitenbeek, Phys. Rev. Lett. 87 (2001) 266102.

[52] L. Vattuone, M. Rocca, P. Restelli, M. Pupo, C. Boragno, U. Valbusa, Phys. Rev. B 49 (1994) 5113.

[53] T. Zambelli, J.V. Barth, J. Wintterlin, Phys. Rev. B 58 (1998) 12663-12666.

[54] T. Hashizume, M. Taniguchi, K. Motai, H. Lu, K. Tanaka, T. Sakurai, Jpn. J. Appl. Phys. 30 (1991) L1529.

[55] W.W. Pai, J.E. Reutt-Robey, Phys. Rev. B 53 (1996) 15997.

[56] M. Taniguchi, K. Tanaka, T. Hashizume, T. Sakurai, Surf. Sci. Lett. 262 (1992) L123-L128.

[57] F. Besenbacher, J.K. Nørskov, Prog. Surf. Sci. 44 (1993) 5-66.

[58] A.G. Sault, R.J. Madix, C.T. Campbell, Surf. Sci. 169 (1986) 347-356.

[59] S. Narasimhan, D. Vanderbilt, Phys. Rev. Lett. 69 (1992) 1564-1567.

[60] S. Helveg, W.X. Li, N.C. Bartelt, S. Horch, E. Lægsgaard, B. Hammer, F. Besenbacher, Phys. Rev. Lett. 98 (2007) 115501.

[61] I. Nakai, Y. Matsumoto, N. Takagi, S. Okazaki, J. Chem. Phys. 129 (2008) 154709.

[62] T. Schimizu, M. Tsukada, Surf. Sci. Lett. 295 (1993) L1017-L1022.

[63] K. Berge, A. Goldmann, Surf. Sci. 540 (2003) 343-354.

[64] J.M. Gottfried, K. Christmann, Surf. Sci. 566 (2004) 1112.

[65] J.M. Gottfried, K.J. Schmidt, S.L.M. Schroeder, K. Christmann, Surf. Sci. 525 (2003) 197.